ELSEVIER

Cryogenics 42 (2002) 299–309

Cryogenics

www.elsevier.com/locate/cryogenics

The unified strain and temperature scaling law for the pinning force density of bronze-route Nb_3Sn wires in high magnetic fields

Najib Cheggour [1], Damian P. Hampshire *

Superconductivity Group, Department of Physics, Science Laboratories, University of Durham, South Road, Durham DH1 3LE, UK

Received 4 December 2001; accepted 14 March 2002

Abstract

Detailed measurements of the critical current density (J_c) of a bronze-route niobium–tin wire are presented for magnetic fields (B) up to 15 T as a function of temperature (T) from 6 K up to 16 K in the strain (ε) range between -0.7% and $+0.7\%$. The data for this technological wire are described by a unified strain and temperature scaling law for the pinning force density of the form $F_p(B,T,\varepsilon) = J_c \times B = A(\varepsilon)[B^*_{c2}(T,\varepsilon)]^n b^p (1-b)^q$, where $A(\varepsilon)$ is a function of strain alone, B^*_{c2} is the effective upper critical field at which F_p extrapolates to zero, $b = B/B^*_{c2}$ is the reduced magnetic field and n, p and q are constants. It is demonstrated that were $A(\varepsilon)(B^*_{c2})^n$ replaced by $F(T)(B^*_{c2})^m$ where $F(T)$ is a function of temperature alone, the strain index m is a strong function of temperature and strain, and in high compression $m = n$. The effective upper critical field can be parameterized using the expression $B^*_{c2}(T,\varepsilon) = B^*_{c2}(0,\varepsilon)(1-(T/T^*_c(\varepsilon))^v)$, where v is a constant and $T^*_c(\varepsilon)$ is the effective critical temperature at which B^*_{c2} at a given strain extrapolates to zero. The strain dependence of the ratio $B^*_{c2}(0,\varepsilon)/T^*_c(\varepsilon)$ and the slope $(-\partial B^*_{c2}(T,\varepsilon)/\partial T)_{T=T^*_c(\varepsilon)}$ is reported. The data presented are useful for cryocooled high field magnets and for identifying the mechanisms that determine J_c in niobium–tin superconducting wires.

Keywords: Superconductors; Critical current density; Flux pinning; Mechanical properties; Critical field; Critical temperature; Strain

1. Introduction

The effect of strain (ε) on the superconducting transition temperature (T_c) and the critical current density (J_c) of niobium–tin (Nb_3Sn) wires and ribbons was first reported in the 1960s [1–3]. It was more than a decade before a substantial effort was directed by the community at understanding the effects of stress and strain on the properties of Nb_3Sn and its ternary compounds [4–21]. It is now widely accepted that the dependence of J_c on strain is primarily associated with changes in the superconductor's fundamental properties such as T_c and the upper critical field B_{c2}, as well as changes in superconductor's microstructure due to strain application.

Among the most challenging design requirements for building electromagnets using Nb_3Sn, which is still the preferred material for applications above 12 T, are those involving electromechanical properties since Nb_3Sn is inherently brittle and the effect of strain on J_c is relatively large in this conductor. The initial increase in J_c with applied tensile strain that is generally observed in Nb_3Sn composites is now well understood as due to the reduction of pre-compression on the superconducting filaments. This pre-compression is applied by other component materials of the composite wire during the cooling from the heat-treatment temperature to the operating temperature due to differential thermal contraction [9,10]. Furthermore, the findings of the Ekin strain scaling law [17] which describes the strain and magnetic field (B) dependence of J_c at 4.2 K, and the Fietz–Webb temperature scaling law [22] which describes the temperature (T) and magnetic field dependence of J_c at zero applied strain, have proven very useful to parameterize J_c for use in the design and fabrication of high magnetic field systems and to provide some insight into the mechanisms that govern J_c in this class of superconductors.

The mechanisms that determine J_c in Nb_3Sn, however, are still not fully understood. This is primarily

* Corresponding author. Tel.: +44-191-374-2184; fax: +44-191-374-3749.

E-mail addresses: cheggour@boulder.nist.gov (N. Cheggour), d.p.hampshire@durham.ac.uk (D.P. Hampshire).

[1] Present address: NIST, Boulder, CO 80305, USA.

0011-2275/02/$ - see front matter
PII: S0011-2275(02)00038-3

because it is not yet clear how normal and superconducting properties vary on the scale of the coherence length which is the scale over which effective flux pinning occurs. There is long standing evidence that in low magnetic fields, grain boundaries are the important pinning sites since $J_c \propto 1/(\text{grain-size})$ [23]. However in high magnetic fields, grain-boundaries probably play a less important role in determining J_c [24–27].

In the last decade, the development of cryocooled and large-scale high field systems has provided additional impetus to extending the strain scaling law to different temperatures. In recent work, we demonstrated that a limited set of $J_c(B,T,\varepsilon)$ data for a bronze processed Nb_3Sn multifilamentary conductor could be described using a unified strain and temperature scaling law [28] of the form first proposed by Kroeger et al. [19]. The law eliminates the apparent inconsistency between the temperature scaling law [22] and the strain scaling law [17]. In this paper, a more comprehensive set of J_c data is presented for a 0.37 mm diameter bronze processed Nb_3Sn multifilamentary wire. In particular, more detailed variable-temperature data are provided and the strain range has been extended so it includes the technologically important range from -0.7% to $+0.7\%$, particularly for development of large-scale systems that utilize cable-in-conduit conductors [29]. These data confirm the applicability of the unified scaling law to a wide temperature and strain range. The effective upper critical field B^*_{c2}, the field at which the pinning force density F_p $(= J_c \times B)$ extrapolates to zero, was found to follow universal scaling as a function of both temperature and strain. Furthermore, the strain dependence of the effective critical temperature T^*_c, the temperature at which B^*_{c2} extrapolates to zero, was extracted from transport J_c data and compared to other data in the literature. The general issues of the parameterization of such data and the implications for the general understanding of J_c in technologically important conductors are also discussed.

2. Experimental procedure

The conductor measured was a bronze-route Vacuumschmelze Nb_3Sn wire 0.37 mm in diameter, which contained 4500 Nb filaments in an unstabilized CuSn matrix. The wire was heat treated on a stainless steel mandrel for 64 h at 700 °C in an argon atmosphere. The wire was then transferred onto a CuBe spring and soldered to it along with current leads and voltage taps.

The probe used to make these measurements has been described in detail elsewhere [30]. Important features include the use of an isolated enclosure which incorporates a CuBe spring on which the sample is mounted [31], high current lead-throughs [32] to enable variable-temperature measurements in vacuum [33], and a copper gasket seal which maintains the vacuum integrity of the probe and sustains the torque applied to the CuBe spring. The spring sample holder, which serves to apply strain to the sample, has the advantage over the end-grip technique with a free standing sample [3,12,17,19] of allowing application of both tensile and compressive strain, and protecting the sample against the Lorentz force produced during the measurements [30,31,34]. The spring technique, however, requires additional measurements or calculations to determine the strain-free state of the sample. The choice of the spring material is critical [30]. CuBe alloy was used in the fabrication of the spring rather than Ti [31] (or Ti coated with Cu and Ag/Cu solder [35]), stainless steel or brass [34,36], because CuBe has a high proportional limit of elasticity, matches the thermal expansion of typical Nb_3Sn technological conductors well and can be soldered to directly [30].

The data acquisition followed standard procedure [30,37–39]. At fixed magnetic field, temperature and strain, the current through the sample was slowly increased and the voltage across the sample measured using a standard four-terminal V–I configuration. The measurement was repeated as a function of magnetic field. Thereafter the temperature was changed and V–I curves measured throughout the field range. Then the strain was changed and V–I curves measured again as a function of field and temperature. This process was repeated at all required strain values to obtain the complete data set. Measurements were made at currents up to ~25 A, from 6 K up to 16 K, in the range of applied strain between -0.7% and $+0.7\%$, in magnetic fields up to 15 T. The shunt resistance parallel to the superconductor, due to the spring sample holder and conductor's matrix, was measured at the normal state (20 K) as a function of magnetic field for three different values of strain. To first order, this resistance is independent of strain and magnetic field. The current sharing through the shunt at 1 μV/cm is as low as 60 mA. Nevertheless it is necessary to take it into account, particularly for the data obtained close to B^*_{c2}. The critical current (I_c) was determined at a criterion of 1 μV/cm after subtracting systematically the current sharing from the V–I curves.

3. Results and analysis

3.1. $J_c(B,T,\varepsilon)$ data and scaling of F_p with magnetic field

The critical current density values (J_c) have been calculated from I_c data using the cross-sectional area of the entire wire. Since this wire contains no copper, the definition of J_c used is equivalent to both the non-copper critical current density and the engineering critical current density of this conductor. Typical J_c data obtained at 12 K as a function of applied strain and magnetic field are shown in Fig. 1. The data confirm that the sample is

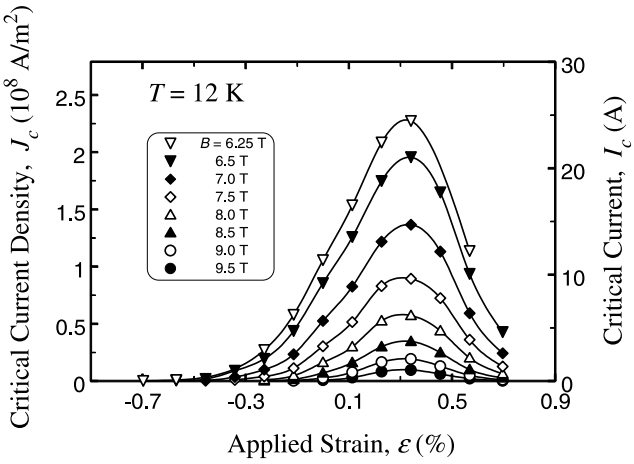

Fig. 1. Critical current density (J_c) data as a function of applied strain (ε) at 12 K for different values of magnetic field (B) using the 1 μV/cm criterion, obtained for a bronze processed Nb_3Sn multifilamentary wire. The position of the peak is situated at around $\varepsilon_{max} = 0.33\%$.

under pre-compression after it has been cooled to cryogenic temperatures, typical of technological Nb_3Sn wires [9,10]. The pre-compressive strain ε_{max} defined by the position of the peak of $J_c(\varepsilon)$, is about 0.33% for this conductor attached to the CuBe spring. In Fig. 2, the same data are plotted in the form of J_c versus magnetic field at different values of applied strain (ε). Note that the application of compressive strain to the sample (as high as −0.7%) offers the possibility of significantly widening the window of study of J_c.

In order to obtain the free parameters in the scaling law equation, a global fitting of all the data was obtained using a field dependence for F_p of the form [22]:

$$F_p = K(T,\varepsilon) b^p (1-b)^q, \quad (1)$$

where $b = B/B^*_{c2}$ is the reduced magnetic field, p and q are constants, and $K(T,\varepsilon)$ is an arbitrary function of temperature and strain. A least-squares fit to the data was made using the subroutine *Solver* available with the software *Microsoft Excel*. The best fit was found for $p = 0.5$ and $q = 3.5$. For comparison we then focussed exclusively on other half-integral values of q: when (p,q) were forced to take the values $(0.5,3)$, the errors increased by a factor of 2.5 with respect to the optimum fit. For $(p,q) = (0.5,2.5)$ the increase was about a factor of 15, while $(p,q) = (0.5,2)$ gave values for B^*_{c2} that were often lower than the magnetic fields at which the supercurrent was measured to be non-zero. In Figs. 3–5,

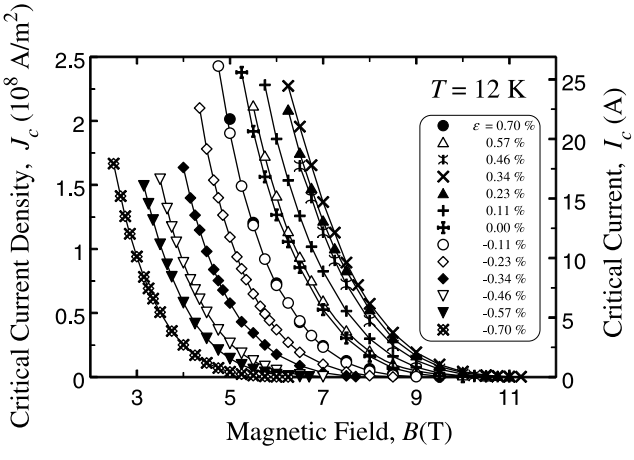

Fig. 2. Critical current density (J_c) data as a function of magnetic field (B) at 12 K for different values of applied strain (ε) using the 1 μV/cm criterion, obtained for a bronze processed Nb_3Sn multifilamentary wire. Application of compressive strain to the sample (as high as −0.7%) offers the possibility of significantly widening the window of study of J_c.

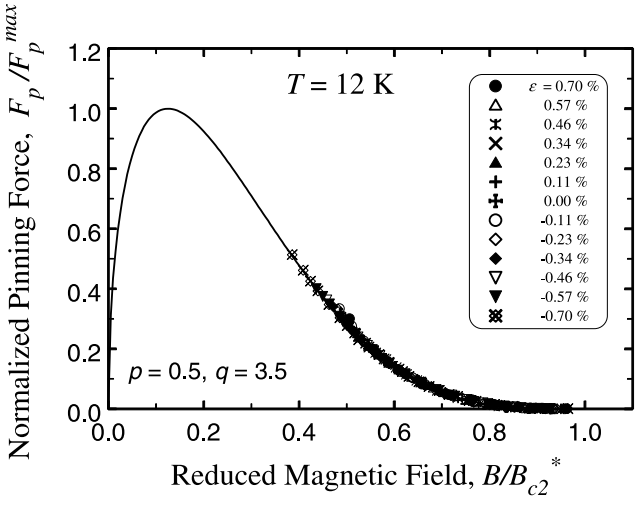

Fig. 3. Normalized pinning force as a function of reduced magnetic field ($b = B/B^*_{c2}$) at 12 K for different values of applied strain (ε), obtained for a bronze processed Nb_3Sn multifilamentary wire. The continuous line represents a function proportional to $b^{0.5}(1-b)^{3.5}$.

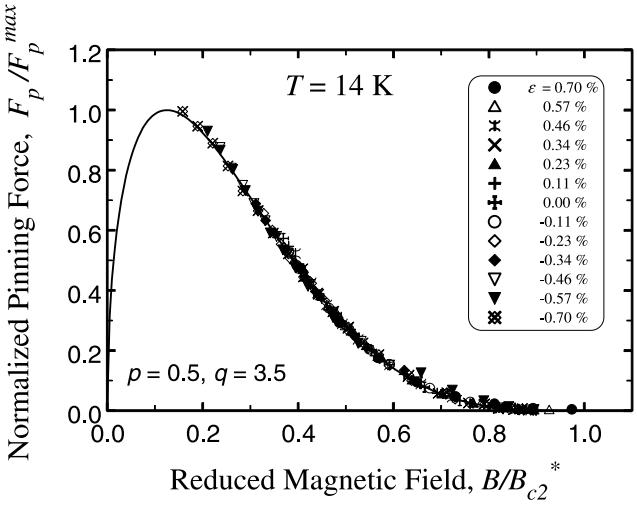

Fig. 4. Normalized pinning force as a function of reduced magnetic field ($b = B/B^*_{c2}$) at 14 K for different values of applied strain (ε), obtained for a bronze processed Nb_3Sn multifilamentary wire. The continuous line represents a function proportional to $b^{0.5}(1-b)^{3.5}$.

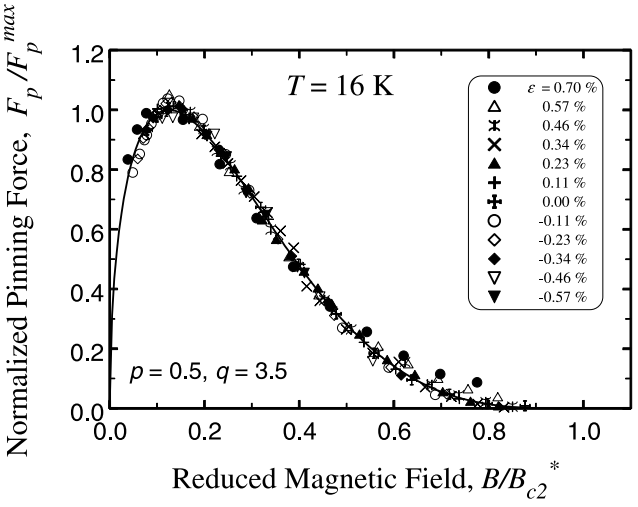

Fig. 5. Normalized pinning force as a function of reduced magnetic field ($b = B/B_{c2}^*$) at 16 K for different values of applied strain (ε), obtained for a bronze processed Nb_3Sn multifilamentary wire. The continuous line represents a function proportional to $b^{0.5}(1-b)^{3.5}$.

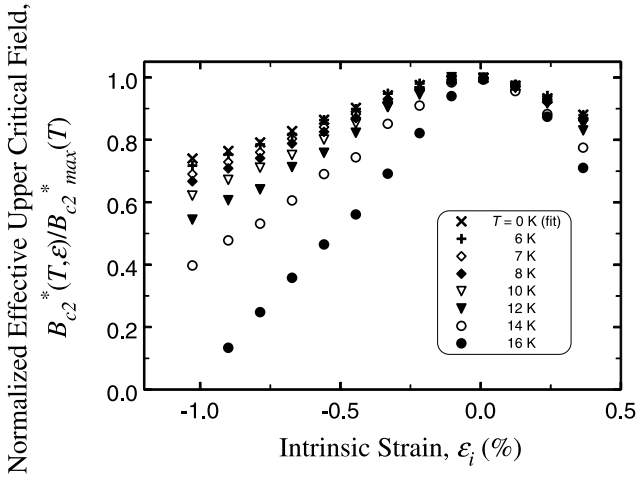

Fig. 6. Normalized effective upper critical field ($B_{c2}^*(T,\varepsilon)/B_{c2\ max}^*(T)$) as a function of intrinsic strain (ε_i) for different values of temperature (T), obtained for a bronze processed Nb_3Sn multifilamentary wire. The data show a systematic increase in the sensitivity of $B_{c2}^*(T,\varepsilon)/B_{c2\ max}^*(T)$ to strain as the temperature is increased. $B_{c2}^*(T,\varepsilon)/B_{c2\ max}^*(T)$ reaches a maximum at zero intrinsic-strain.

good scaling of the data at 12, 14 and 16 K is shown using the values $p = 0.5$ and $q = 3.5$. The scaling of F_p with magnetic field is observed for all the values of strain and temperature used.

3.2. Universal scaling of B_{c2}^* with strain and temperature

Values of the effective upper critical field ($B_{c2}^*(T,\varepsilon)$) were determined from the data fitting procedure described above. In light of the enormous effort directed at understanding the phase diagram for the flux-line-lattice of high temperature superconductors [40–42], one may consider whether $B_{c2}^*(T,\varepsilon)$ is, for example, characteristic of a distribution of superconducting parameters [43–46] or a flux-lattice melting [47–51]. Additional extended measurements of V–I characteristics over a broader range of voltages are required to address these questions properly.

In Fig. 6, the normalized field $B_{c2}^*(T,\varepsilon)/B_{c2\ max}^*(T)$ is shown at different temperatures as a function of intrinsic strain $\varepsilon_i = \varepsilon - \varepsilon_{max}$ (where ε is the applied strain). The data show a systematic increase in the sensitivity of $B_{c2}^*(T,\varepsilon)/B_{c2\ max}^*(T)$ to strain as the temperature is increased, confirming the results previously reported for a limited temperature range [28]. In Fig. 7, B_{c2}^* is plotted as a function of temperature for different values of applied strain. The solid lines in the figure are given by

$$B_{c2}^*(T,\varepsilon) = B_{c2}^*(0,\varepsilon)\left(1-\left(\frac{T}{T_c^*(\varepsilon)}\right)^{v}\right), \qquad (2)$$

where $B_{c2}^*(0,\varepsilon)$ is the effective upper critical field at 0 K, $T_c^*(\varepsilon)$ is the effective critical temperature at which $B_{c2}^*(T,\varepsilon)$ extrapolates to zero, and v is a constant. For

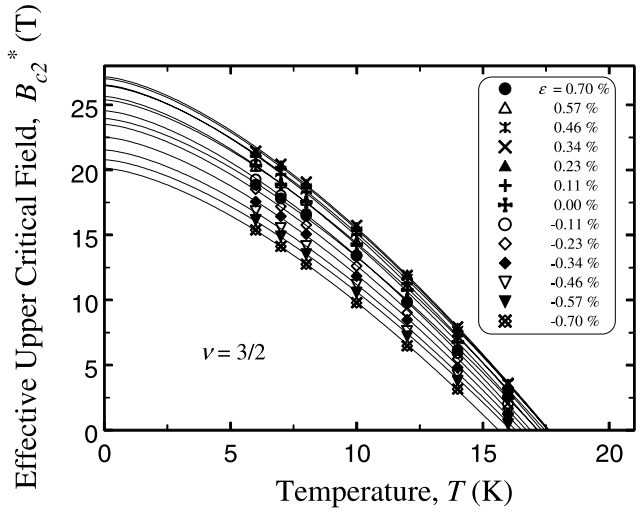

Fig. 7. Effective upper critical field ($B_{c2}^*(T,\varepsilon)$) as a function of temperature (T) and applied strain (ε), obtained for a bronze processed Nb_3Sn multifilamentary wire. The solid lines represent the function $B_{c2}^*(T,\varepsilon) = B_{c2}^*(0,\varepsilon)(1-(T/T_c^*(\varepsilon))^v)$, where the exponent $v = 3/2$.

the data presented here, the optimum fit is found for $v = 3/2$. As presented in Fig. 8, $B_{c2}^*(T,\varepsilon)$ data follow a universal scaling law as a function of both temperature and strain. This result shows that $B_{c2}^*(T,\varepsilon)$ values can be predicted for any temperature and strain from a limited number of measurements. By measuring $B_{c2}^*(\varepsilon)$ at a given temperature (4.2 K for example) and $T_c^*(\varepsilon)$, $B_{c2}^*(T,\varepsilon)$ values can be calculated using Eq. (2).

From the derivative of Eq. (2) with respect to temperature, one can write an expression for $B_{c2}^*(0,\varepsilon)$ as a function of $T_c^*(\varepsilon)$ and the slope of $B_{c2}^*(T,\varepsilon)$ near $T_c^*(\varepsilon)$:

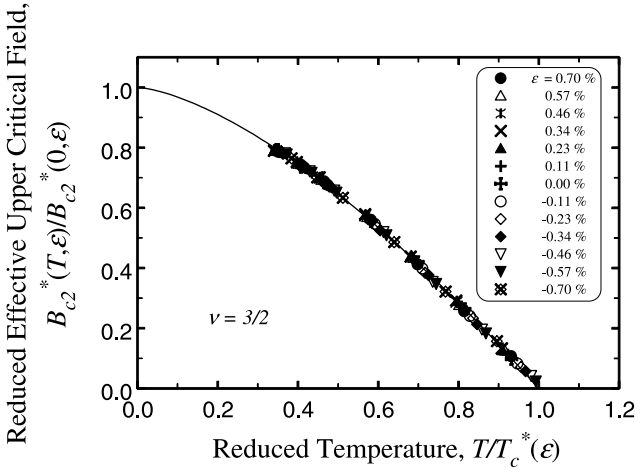

Fig. 8. Reduced effective upper critical field ($B_{c2}^*(T,\varepsilon)/B_{c2}^*(0,\varepsilon)$) as a function of reduced temperature ($T/T_c^*(\varepsilon)$) and applied strain (ε), obtained for a bronze processed Nb_3Sn multifilamentary wire. The solid line represents the function $B_{c2}^*(T,\varepsilon) = B_{c2}^*(0,\varepsilon)(1-(T/T_c^*(\varepsilon))^{\nu})$, where the exponent $\nu = 3/2$. The data show a universal scaling of $B_{c2}^*(T,\varepsilon)$ as a function of both temperature and strain.

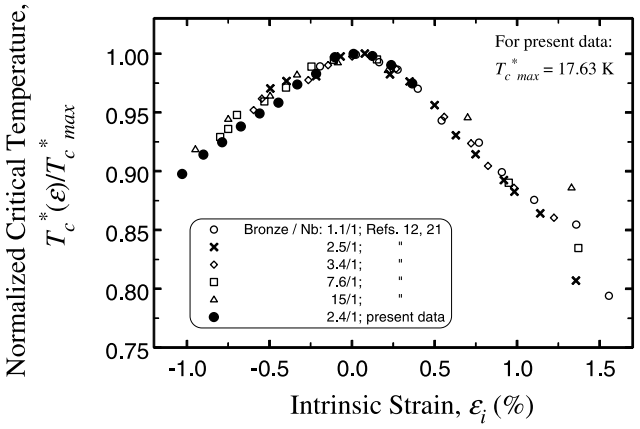

Fig. 10. Normalized effective critical temperature ($T_c^*(\varepsilon)/T_{c\max}^*$) as a function of intrinsic strain (ε_i), obtained for a bronze processed Nb_3Sn multifilamentary wire. Also presented are normalized critical temperature data, inductively measured for a series of monofilamentary Nb_3Sn conductors with different bronze to niobium ratios [12,21]. The data show a universal strain dependence for T_c^* (or T_c), as reported previously [17,21] for Nb_3Sn wires. $T_c^*(\varepsilon)/T_{c\max}^*$ reaches a maximum at zero intrinsic-strain.

$$B_{c2}^*(0,\varepsilon) = -\frac{2}{3}T_c^*(\varepsilon)\left(\frac{\partial B_{c2}^*(T,\varepsilon)}{\partial T}\right)_{T=T_c^*(\varepsilon)}. \quad (3)$$

The factor $2/3$ ($= \nu^{-1}$) in Eq. (3) is consistent with that calculated in WHH theory (=0.693) for a dirty superconductor with no Pauli paramagnetic limiting [52].

In Figs. 9 and 10, $B_{c2}^*(0,\varepsilon)$ and $T_c^*(\varepsilon)$ values obtained from data fitting using Eq. (2) are plotted as a function of intrinsic strain. The present $T_c^*(\varepsilon)$ data, which were extracted from transport J_c measurements, are compared to other results in the literature obtained for monofilamentary Nb_3Sn wires with different bronze to niobium ratios using ac susceptibility technique [12,21]. Fig. 10 shows that there is a clear similarity in the intrinsic strain dependence of the critical temperature for the different conductors. This universal strain dependence of T_c has been observed before [17,21] for Nb_3Sn wires. The fact that the present $T_c^*(\varepsilon)$ data also fall onto this universal curve suggests that the universal strain dependence of T_c (or T_c^*) may not be very dependent on the technique of measurement. All $J_c(B,T,\varepsilon)$, $B_{c2}^*(T,\varepsilon)$ and $T_c^*(\varepsilon)$ data obtained have a peak located at the same strain value $\varepsilon_{\max} = 0.33\%$, demonstrating a correlation between the variables J_c, B_{c2}^* and T_c^*.

In Fig. 11, the ratio $B_{c2}^*(0,\varepsilon)/T_c^*(\varepsilon)$ is plotted as a function of intrinsic strain. This ratio is found to be strain dependent. The relatively high values of $B_{c2}^*(0,\varepsilon)$ and $T_c^*(\varepsilon)$ suggest that they are not too far below the equivalent thermodynamic parameters. The thermodynamic

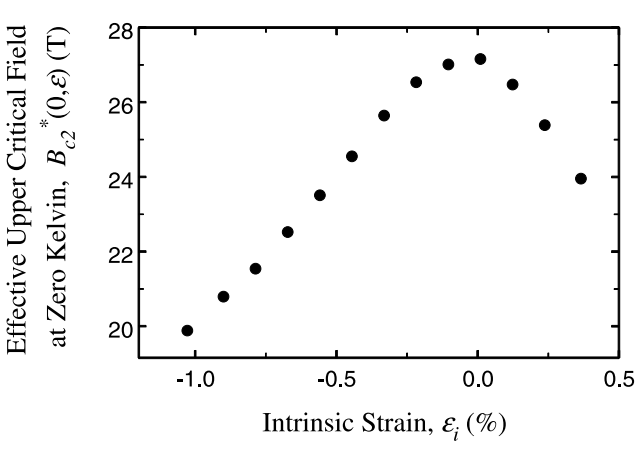

Fig. 9. Extrapolated effective upper critical field at 0 K ($B_{c2}^*(0,\varepsilon)$) as a function of intrinsic strain (ε_i), obtained for a bronze processed Nb_3Sn multifilamentary wire. $B_{c2}^*(0,\varepsilon)$ reaches a maximum at zero intrinsic-strain.

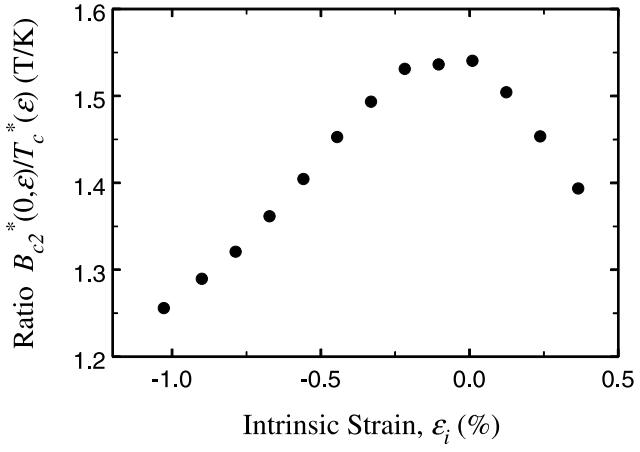

Fig. 11. Ratio $B_{c2}^*(0,\varepsilon)/T_c^*(\varepsilon)$ of the extrapolated effective upper critical field at 0 K over the effective critical temperature, as a function of intrinsic strain obtained for a bronze processed Nb_3Sn multifilamentary wire. This ratio reaches a maximum at zero intrinsic-strain.

relationship between the upper critical field at 0 K and the critical temperature in the dirty limit is given by [53]

$$B_{c2}(0) = 3 \times 10^4 \gamma \rho_n T_c, \tag{4}$$

where γ is the Sommerfeld constant and ρ_n is the residual resistivity in the normal conducting state. If one assumes there is little difference between the fitting parameters and the thermodynamic parameters [54,55], one can expect the change in density of electronic states due to strain application to affect both γ and T_c^* and, therefore, the ratio $B_{c2}^*(0,\varepsilon)/T_c^*(\varepsilon)$ to depend on strain.

The slope $\left(-\partial B_{c2}^*(T,\varepsilon)/\partial T\right)_{T=T_c^*(\varepsilon)}$, calculated from the ratio $B_{c2}^*(0,\varepsilon)/T_c^*(\varepsilon)$ using Eq. (3), varies between 1.88 and 2.31 T/K for the strain range we investigated. It is interesting to notice that these values are consistent with those reported by Orlando et al. [56] for the slope of the upper critical field of Nb_3Sn material near T_c.

3.3. Unified strain and temperature scaling law for F_p

From the values of $K(T,\varepsilon)$, p and q found from the data fitting, the maximum value of the volume pinning force density $F_p^{max}(T,\varepsilon)$ has been calculated at every temperature and strain. In Fig. 12, $F_p^{max}(T,\varepsilon)$ is plotted versus $B_{c2}^*(T,\varepsilon)$. At each strain, the gradient of the corresponding line has been calculated and is plotted in Fig. 13. This gradient (n) is reasonably constant with an average value over the strain range measured of about 3.24 and a slight tendency to increase at high compressive strain as found in previous work [28]. This weak dependence of the gradient (i.e. n) on strain found for this technological conductor was also observed by Kroeger et al. for a model Nb_3Sn monofilament [19]. This result implies that the volume pinning force density is given by

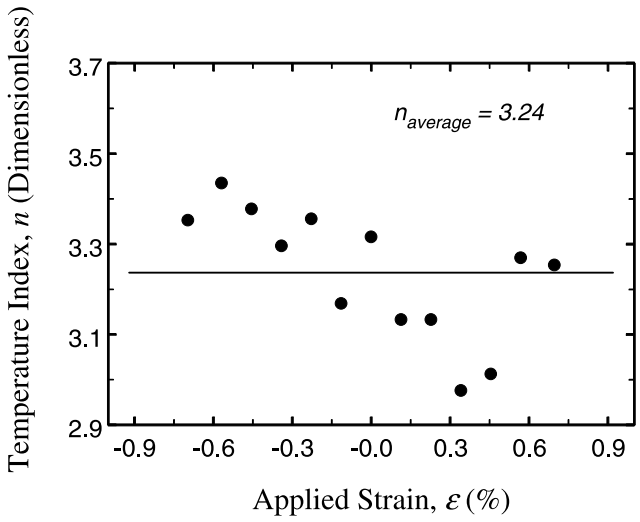

Fig. 13. Temperature index (n) as a function of applied strain (ε) of bronze processed Nb_3Sn multifilamentary wire. The average value of n is about 3.24.

$$F_p(B,T,\varepsilon) = J_c \times B = A(\varepsilon)[B_{c2}^*(T,\varepsilon)]^n b^p (1-b)^q, \tag{5}$$

where $A(\varepsilon)$ is a function of strain alone, B_{c2}^* is the effective upper critical field, $b = B/B_{c2}^*$ the reduced magnetic field, $n = 3.24$, $p = 0.5$ and $q = 3.5$. The parameter n is called the temperature index because it is the exponent found when the strain is fixed and the scaling law measured as a function of temperature. Typical values for n are in the range 2–4 for low temperature superconductors including NbTi [22,57,58], Nb_3Sn [19,28,59], Nb_3Al [60], V_3Ga [61], NbN [62] and $PbMo_6S_8$ [63–66]. The prefactor $A(\varepsilon)$ is presented in Fig. 14 where the value of n has been taken to be 3.24. The shape of $A(\varepsilon)$, particularly at high compressive strain, is discussed below. The value of n has also been recalculated for a restricted strain range $-0.2\% \leqslant \varepsilon \leqslant +0.7\%$ and found to

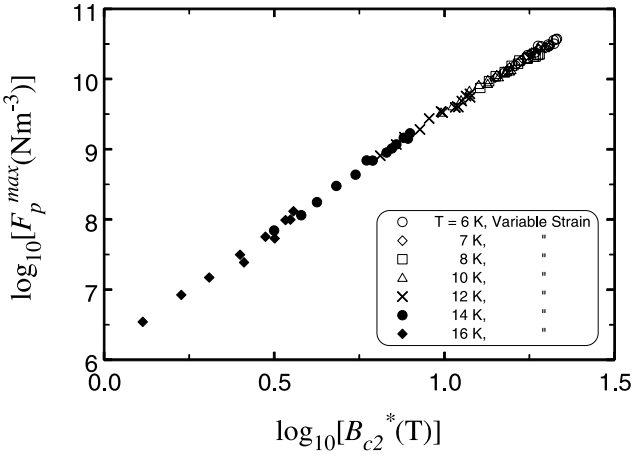

Fig. 12. Plots of $\log_{10}(F_p^{max})$ versus $\log_{10}(B_{c2}^*)$ for different values of temperature (T) and applied strain (ε), obtained for a bronze processed Nb_3Sn multifilamentary wire.

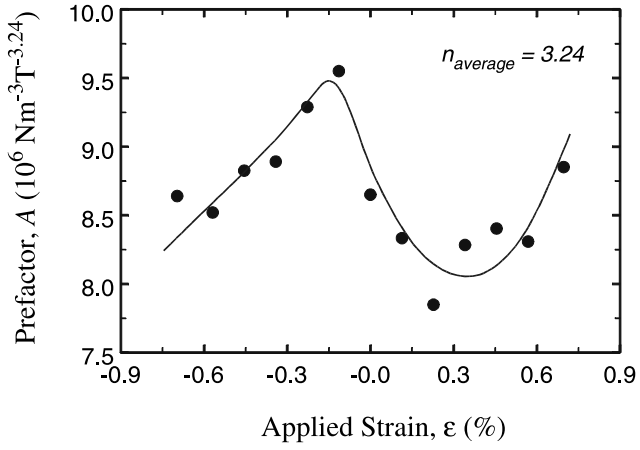

Fig. 14. Prefactor A as a function of applied strain of bronze processed Nb_3Sn multifilamentary wire, for $n = 3.24$. A is defined by the equation $F_p(B,T,\varepsilon) = J_c \times B = A(\varepsilon)[B_{c2}^*(T,\varepsilon)]^n b^p (1-b)^q$.

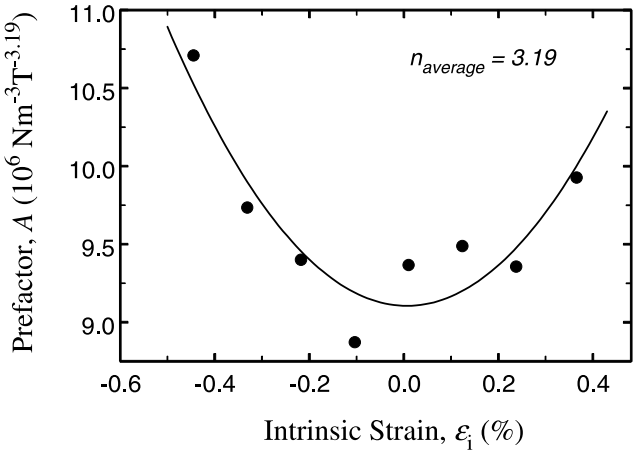

Fig. 15. Prefactor A as a function of intrinsic strain (ε_i) of bronze processed Nb_3Sn multifilamentary wire, corresponding to an average value $n = 3.19$ calculated for a restricted range of applied strain (ε) between $-0.2\% \leqslant \varepsilon \leqslant +0.7\%$. $A(\varepsilon)$ reaches a minimum at about zero intrinsic-strain, where T_c^*, B_{c2}^* and J_c go through a maximum.

be about 3.19. In Fig. 15, the equivalent values of $A(\varepsilon)$ are presented as a function of intrinsic strain. These data can be fitted by a smooth inverted parabola and show a minimum at the strain ε_{max} where J_c, B_{c2}^* and T_c^* reach their maxima, consistent with previous results [28] (see Fig. 17) and those of Kroeger et al. [19,67].

We have also investigated how the data can be described using the strain scaling law formulation [17]. The term $A(\varepsilon)(B_{c2}^*)^n$ in Eq. (5) was replaced by $F(T)(B_{c2}^*)^m$ where $F(T)$ is a function of temperature alone and m is the strain index. In Fig. 16, m is plotted as a function of temperature when calculated in two different strain ranges. The strain index is a strong function of temperature and strain. For relatively small intrinsic strains, m can be parameterized by the linear relation $m = 0.23T$. The data presented are consistent with Ekin's data [17] since at 4.2 K the value of m extrapolates to approximately 1. For strong compressive strains, we note that m is nearly equal to the temperature index n found in Eq. (5). Although the strain index can be useful for parameterizing data at fixed temperature (e.g. 4.2 K), we conclude that there is no simple unified description of the data over the complete magnetic field, temperature and strain range if it is assumed that A has no strain dependence.

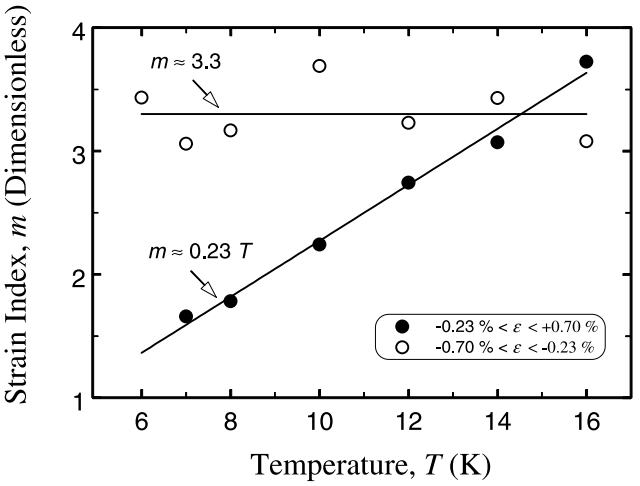

Fig. 16. Strain index (m) as a function of temperature in different applied strain (ε) ranges, obtained for a bronze processed Nb_3Sn multifilamentary wire. In general, the index m is a function of temperature and strain. For relatively small intrinsic strains, m is a linear function of temperature. In the high compressive strain range, m has approximately the same value as the temperature index n.

4. Discussion

The finding by Fietz and Webb [22] of systematic scaling of the bulk pinning force density with temperature and magnetic field in a series of superconducting niobium alloys was an important step towards a better understanding of flux pinning mechanisms in hard superconductors. Subsequently, the observation by Ekin of strain scaling and magnetic field scaling of F_p in a wide range of technological conductors at 4.2 K [17,68] extended the idea of scaling to include strain, which is a crucial parameter from technological applications standpoint. The strain scaling law became a useful tool for designing relatively small superconducting magnets to operate at ~4.2 K. The difference in the dependence of F_p on B_{c2}^* found in the temperature scaling law and the strain scaling law, however, required additional experimental study to elucidate this point.

Work by Kroeger et al. [19] on a model bronze-route Nb_3Sn monofilament with a very large bronze to niobium ratio of 34 to 1 demonstrated that the simple flux pinning semi-empirical scaling law of the form of Eq. (1) described both the temperature scaling and strain scaling of the pinning force density. Given that only tensile strain could be applied in these experiments, the purpose-built conductor was designed to put the monofilament under a large thermal pre-compression after cooling, to increase the strain range over which J_c could be investigated. F_p scaled with magnetic field using B_{c2} values determined from the low temperature side of complementary resistive transition data, although this scaling was not confirmed for all the samples measured over the whole range of strain and temperature. Kroeger and co-workers proposed that the prefactor A in the Fietz–Webb temperature scaling law depends on strain. This dependence represents an additional effect of strain on J_c, independent of that due to the variation of B_{c2} and T_c with strain.

In previous work, we demonstrated that the apparent inconsistency between the dependence of F_p on B_{c2}^* found in the temperature scaling law [22] and the strain

scaling law at 4.2 K [17] is removed using the unified strain and temperature scaling law formulated in Eq. (5). In this work, we have extended the measurements to a larger strain range and provided additional detailed variable-temperature measurements of J_c in high magnetic fields. Systematic scaling of F_p with temperature, strain, and magnetic field using B^*_{c2} values is observed, and a correlation between the variables J_c, B^*_{c2} and T^*_c is demonstrated. Furthermore, universal scaling of $B^*_{c2}(T,\varepsilon)$ with both temperature and strain was found. These data demonstrate that the unified strain and temperature scaling law of F_p is not only valid for a purpose-built monofilament conductor, but also for a technological Nb_3Sn wire throughout the entire technologically important temperature and strain range in magnetic fields.

Additional fundamental parameters, such as the Ginzburg–Landau parameter (κ) [59,69,70] and the thermodynamic critical field (H_c) [71] may be required for a complete description of flux pinning. However until the strain, temperature, microstructural and compositional dependence of these parameters is known, it remains challenging to include them. The strain dependence of the fundamental and microstructural parameters, that are not yet included in the unified scaling law, may also contribute to the strain dependence of the prefactor A. Hence we suggest that the status of A is currently just a fitting parameter so a smooth functional form is all one can expect. Furthermore, as the prefactor A is mainly related to the microstructure of the sample [19,28], one may expect $A(\varepsilon)$ to vary from conductor to conductor. The amplitude and variation with strain of A for the sample studied in this work is very similar to that of a sister sample we investigated previously (Fig. 17) [28], but noticeably different from the data reported by Kroeger et al. [19] on a highly pre-compressed monocore Nb_3Sn conductor. The total variation of $A(\varepsilon)$ for our conductor is about 20%, compared to about 150% for the monocore conductor [19]. As the prefactor A and B_{c2} (or B^*_{c2}) have opposite effects on J_c, the relatively high sensitivity of A to strain for the conductor studied by Kroeger et al. could be the reason for the peak value of $J_c(\varepsilon)$ not occurring at the same strain as for $B_{c2}(\varepsilon)$ and $T_c(\varepsilon)$ [19]. For the conductor investigated in this work and in previous work [28], the correlation between the variables J_c, B^*_{c2} and T^*_c observed may be linked to the relatively small sensitivity of A to strain. Despite this relatively small sensitivity for the sample we investigated, $A(\varepsilon)$ data can be fitted by a smooth inverted parabola over a range of strain around ε_{max} (Fig. 15). The origin of the deviation from this dependence of $A(\varepsilon)$ that we have observed in high compressive regime at around an intrinsic strain $\varepsilon_i \approx -0.5\%$ (Fig. 14) is a source of speculation at present, but may be due to a stress-induced structural phase transition [8,21].

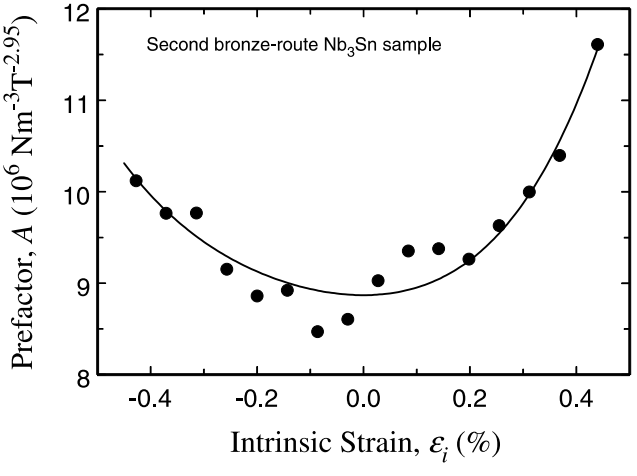

Fig. 17. Prefactor A as a function of intrinsic strain (ε_i) of a second bronze processed Nb_3Sn sample investigated in Ref. [28]. $A(\varepsilon)$ reaches a minimum at about zero intrinsic-strain, where T^*_c, B^*_{c2} and J_c go through a maximum. The amplitude and variation with strain of A for this sample is very similar to that of the sample investigated in the present work (Fig. 15).

One noticeable similarity between the data in this work, our previous work [28] and Kroeger's work [19], is the value of the temperature index n, which is about 3. The value of the parameter p seems to be optimum at around 0.5. The parameter q in the present work is somewhat high compared to the Kramer model or the flux-line-shear-model predictions ($q = 2$) [69], although q values as high as 3 have been reported for Nb_3Sn conductors [19]. It has been suggested that large values of the parameter q can be associated with a distribution in the upper critical field at the grain boundaries [72,73]. A Kramer extrapolation to determine B^*_{c2} (assuming $p = 0.5$ and $q = 2$) [69] does not seem to work for all technological Nb_3Sn conductors, and may result in an overestimation or underestimation of B^*_{c2}. As the parameters p and q may vary from sample to sample of the same conductor depending on metallurgical and thermal processing [69], it is probably best to consider them as free fitting parameters.

In magnet applications, the Lorentz force applied to the windings radially generates a hoop stress that can be transformed into two stress components: axial tension and transverse compression. Besides axial strain, transverse compressive stress has also been reported to have an effect on J_c [74–77], which demonstrates the tensorial nature of the strain state [20]. Some work has emphasized the role of deviatoric strain in changing the superconducting properties [21,34,36,78]. However, it is not clear to what degree the hydrostatic strain component can be neglected. A full description of the pinning force density as a function of tensorial strain, temperature and magnetic field would be useful for an optimum design of large-scale magnets.

5. Conclusion

Scaling of the pinning force density with strain, temperature and magnetic field has been confirmed over an extended temperature and strain range for a technological bronze processed Nb_3Sn multifilamentary wire. The data are described with the unified strain and temperature scaling law of the form $F_p(B,T,\varepsilon) = J_c \times B = A(\varepsilon)[B^*_{c2}(T,\varepsilon)]^n b^p (1-b)^q$. If one replaces $A(\varepsilon) \times (B^*_{c2})^n$ by $F(T)(B^*_{c2})^m$ in this equation, the strain index m is a strong function of temperature and strain. In the high compressive strain range, m approaches the same value as the temperature index n. In the technological conductor investigated, the strain dependent prefactor $A(\varepsilon)$ reaches a minimum at zero intrinsic-strain where T^*_c, B^*_{c2} and J_c go through their maxima. At high compressive strains, $A(\varepsilon)$ deviates from a smooth inverted parabola and no simple parameterization of $A(\varepsilon)$ was possible over the whole strain range. This deviation may in part be due to a stress-induced structural phase transformation.

A universal scaling of $B^*_{c2}(T,\varepsilon)$ with both temperature and strain was found. The effective upper critical field can be described using the expression

$$B^*_{c2}(T,\varepsilon) = B^*_{c2}(0,\varepsilon)\left(1 - \left(\frac{T}{T^*_c(\varepsilon)}\right)^{3/2}\right).$$

Furthermore, the effective critical temperature is found to follow similar universal strain dependence of inductively measured T_c, reported in the literature for various Nb_3Sn wires. Finally, the ratio $B^*_{c2}(0,\varepsilon)/T^*_c(\varepsilon)$ and the slope $(-\partial B^*_{c2}(T,\varepsilon)/\partial T)_{T=T^*_c(\varepsilon)}$ are found to depend on strain.

Acknowledgements

The authors wish to thank: C. Walters and C. Baynham for the benefit of their experience with the Walters probe; G. Teasdale and P. Armstrong in the construction of the probe; T.P.A. Hase for help in fitting the data; J.W. Ekin, H. Jones, S. Keys, and C.M. Friend for very useful discussions. N. Cheggour and G. Teasdale were funded by EPSRC (UK) GR/K70854. D.P. Hampshire was funded as an advanced EPSRC Fellow AF/100409.

References

[1] Müller CB, Saur EJ. Influence of mechanical constraints on the superconducting transition of Nb_3Sn-coated niobium wires and ribbons. Adv Cryog Eng 1962;8:574.

[2] Müller CB, Saur EJ. Influence of mechanical constraints on critical currents of superconducting surface layers of Nb_3Sn on niobium and V_3Ga on vanadium in transverse magnetic fields. Adv Cryog Eng 1964;9:338.

[3] Buehler E, Levinstein HJ. Effect of tensile stress on the transition temperature and current-carrying capacity of Nb_3Sn. J Appl Phys 1965;36:3856.

[4] Luhman T, Suenaga M. Effects of stresses, induced by thermal contraction of a bronze matrix, on the superconducting properties of Nb_3Sn wires. Appl Phys Lett 1976;29(1):61.

[5] Ekin JW. Effect of stress on the critical current of Nb_3Sn multifilamentary composite wire. Appl Phys Lett 1976;29(3):216.

[6] Easton DS, Schwall RE. Performance of multifilamentary Nb_3Sn under mechanical load. Appl Phys Lett 1976;29(5):319.

[7] Ekin JW. Mechanisms for critical-current degradation in NbTi and Nb_3Sn filamentary wires. IEEE Trans Magn 1977;13(1):127.

[8] Luhman T, Suenaga M. The influence of thermally induced matrix stresses on the superconducting properties of Nb_3Sn wire conductors. IEEE Trans Magn 1977;13(1):800.

[9] Hillmann H, Kuckuck H, Pfister H, Rupp G, Springer E, Wilhelm M, et al. Properties of multifilamentary Nb_3Sn conductors. IEEE Trans Magn 1977;13(1):792.

[10] Rupp G. Enhancement of the critical current of multifilamentary Nb_3Sn conductors by tensile stress. J Appl Phys 1977;48(9):3858.

[11] Koch CC, Easton DS. A review of mechanical behaviour and stress effects in hard superconductors. Cryogenics 1977;17:391.

[12] Luhman T, Suenaga M, Klamut CJ. Influence of tensile stresses on the superconducting temperature of multifilamentary Nb_3Sn composite conductors. Adv Cryog Eng 1978;24:325.

[13] Easton DS, Kroeger DM. Kirkendall voids: A detriment to Nb_3Sn superconductors. IEEE Trans Magn 1979;15(1):178.

[14] Rupp G. Stress induced normal-superconducting transition in multifilamentary Nb_3Sn conductors. IEEE Trans Magn 1979;15(1):189.

[15] Barlett RJ, Taylor RD, Thompson JD. Stress effects on multifilamentary Nb_3Sn wire. IEEE Trans Magn 1979;15(1):193.

[16] Ekin JW. Strain dependence of the critical current and critical field in multifilamentary Nb_3Sn composites. IEEE Trans Magn 1979;15(1):197.

[17] Ekin JW. Strain scaling law for flux pinning in practical superconductors. Part I: Basic relationship and application to Nb_3Sn conductors. Cryogenics 1980;20:611.

[18] Ekin JW. Strain scaling law and the prediction of uniaxial and bending strain effects in multifilamentary superconductors. In: Proceedings of the ICMC on Filamentary A15 Superconductors. New York: Plenum Press; 1980. p. 187.

[19] Kroeger DM, Easton DS, DasGupta A, Koch CC, Scarbrough JO. The effect of strain upon the scaling law for flux pinning in bronze process Nb_3Sn. J Appl Phys 1980;51(4):2184.

[20] Scanlan RM, Hoard RW, Cornish DN, Zbasnik JP. Mechanical properties of high-current multifilamentary Nb_3Sn conductors. In: Proceedings of the ICMC on Filamentary A15 Superconductors. New York: Plenum Press; 1980. p. 221.

[21] Welch DO. Alteration of the superconducting properties of A15 compounds and elementary composite superconductors by nonhydrostatic elastic strain. Adv Cryog Eng 1980;26:48.

[22] Fietz WA, Webb WW. Hysteresis in superconducting alloys—Temperature and field dependence of dislocation pinning in niobium alloys. Phys Rev 1969;178(2):657.

[23] Schauer W, Schelb W. Improvement of Nb_3Sn high field critical current by a two-stage reaction. IEEE Trans Magn 1981;17(1):374.

[24] Suenaga M, Tsuchiya K, Higuchi N, Tachikawa K. Superconducting critical-current densities of commercial multifilamentary Nb_3Sn(Ti) wires made by the bronze process. Cryogenics 1985;25:123.

[25] Kramer EJ. Microstructure—Critical current relationships in hard superconductors. J Electron Mater 1975;4(5):839.

[26] Osborne KE, Kramer EJ. The influence of plastic deformation on the peak effect in a type II superconductor. Philos Mag 1974;29: 685.
[27] Banno N, Takeuchi T, Itoh K, Wada H, Matsumoto H, Tachikawa K. Pinning characteristics of $(Nb,Ta)_3Sn$ superconductors produced by Nb/Ta–Sn composite process. IEEE Trans Appl Supercond 2001;11(1):3696.
[28] Cheggour N, Hampshire DP. Unifying the strain and temperature scaling laws for the pinning force density in superconducting niobium–tin multifilamentary wires. J Appl Phys 1999;86(1): 552.
[29] ten Haken B, Godeke A, ten Kate HHJ, Specking W. The critical current of Nb_3Sn wires for ITER as a function of the axial tension and compression. IEEE Trans Magn 1996;32(4):2739.
[30] Cheggour N, Hampshire DP. A probe for investigating the effects of temperature, strain and magnetic field on transport critical currents in superconducting wires and tapes. Rev Sci Instrum 2000;71(12):4521.
[31] Walters CR, Davidson IM, Tuck GE. Long sample high sensitivity critical current measurements under strain. Cryogenics 1986;26:406.
[32] Mathu F, Meijer HC. Some electrical feedthroughs to be used at low temperature. Cryogenics 1982;22:428.
[33] Friend CM, Hampshire DP. A probe for the measurement of the transport critical current density of superconductors in high magnetic fields and at temperatures between 2 and 150 K. J Meas Sci Technol 1995;6:98.
[34] ten Haken B. Strain effects on the critical properties of high-field superconductors. PhD thesis, University of Twente, 1994.
[35] Godeke A, Krooshoop HJG, Knoopers HG, ten Haken B, ten Kate HHJ. Experimental verification of the temperature and strain dependence of the critical properties in Nb_3Sn wires. IEEE Trans Appl Supercond 2001;11(1):1526.
[36] ten Haken B, Godeke A, ten Kate HHJ. The influence of compressive and tensile axial strain on the critical properties of Nb_3Sn Conductors. IEEE Trans Appl Supercond 1995;5(2): 1909.
[37] Goodrich LF, Vecchia DF, Pittman ES, Ekin JW, Clark AF. Critical current measurements on an NbTi superconducting wire standard reference material. NBS special publication no. 260-91, 1984.
[38] Critical current measurement—DC critical current of Nb_3Sn composite superconductors. IEC 61788-2, 1999.
[39] Keys S, Hampshire DP. Testing of conductors. In: Cardwell D, Ginley D, editors. Handbook of superconducting materials. Institute of Physics, Bristol, in press.
[40] Brandt EH. The flux-line lattice in superconductors. Rep Prog Phys 1995;58:1465.
[41] Cohen LF, Jenson HJ. Open questions in the magnetic behaviour of high-temperature superconductors. Rep Prog Phys 1997;60: 1581.
[42] Blatter G, Feigel'man MV, Geshkenbein VB, Larkin AI, Vinokur VM. Vortices in high-temperature superconductors. Rev Mod Phys 1994;66(4):1125.
[43] Yeshurun Y, Malozemoff AP. Giant flux creep and irreversibility in an Y–Ba–Cu–O crystal: an alternative to the superconducting-glass model. Phys Rev Lett 1988;60:2202.
[44] Sun JZ, Eom CB, Lairson B, Bravman JC, Geballe TH. Magnetic relaxation, current–voltage characteristics, and possible dissipation mechanisms for high-T_c superconducting thin films of Y–Ba–Cu–O. Phys Rev B 1991;43(4):3002.
[45] Hampshire DP, Jones H. Analysis of the general structure of the *E–I* characteristic of high current superconductors with particular reference to a NbTi SRM wire. Cryogenics 1987;27:608.
[46] Kiss T, Matsushita T, Irie F. Relationship among flux depinning, irreversibility and phase transition in a disordered HTS material. Supercond Sci Technol 1999;12:1079.
[47] Koch RH, Foglietti V, Gallagher WJ, Koren G, Gupta A, Fisher MPA. Experimental evidence for vortex-glass superconductivity in Y–Ba–Cu–O. Phys Rev Lett 1989;63(14):1511.
[48] Nelson DR, Seung HS. Theory of melted flux liquids. Phys Rev B 1989;39(13):9153.
[49] Houghton A, Pelcovits RA, Sudbø A. Flux lattice melting in high-T_c superconductors. Phys Rev B 1989;40(10):6763.
[50] Tinkham M. Introduction to the phenomenology of high temperature superconductors. Physica C 1994;235:3.
[51] Franz M, Teitel S. Vortex-lattice melting in two-dimensional superconducting networks and films. Phys Rev B 1995;51(10): 6551.
[52] Werthamer NR, Helfand E, Hohenberg PC. Temperature and purity dependence of the superconducting critical field, H_{c2}. III. Electron spin and spin-orbit effects. Phys Rev 1966;147(1): 295.
[53] Goodman BB. Type II superconductors. Rep Prog Phys 1966;29:445.
[54] Suenaga M, Ghosh AK, Xu Y, Welch DO. Irrerversibility temperatures of Nb_3Sn and NbTi. Phys Rev Lett 1991;66(13): 1777.
[55] Daniel IJ, Hampshire DP. Harmonic calculations and measurements of the irreversibility field using a vibrating sample magnetometer. Phys Rev B 2000;61(10):6982.
[56] Orlando TP, McNiff Jr. EJ, Foner S, Beasley MR. Critical fields, Pauli paramagnetic limiting, and material parameters of Nb_3Sn and V_3Si. Phys Rev B 1979;19(9):4545.
[57] Cooley LD, Lee PJ, Larbalestier DC. Is magnetic pinning a dominant mechanism in Nb–Ti? IEEE Trans Magn 1991;27(2): 1096.
[58] Friend CM, Hampshire DP. Transverse and longitudinal critical current densities in Nb46wt%Ti multifilamentary wire from 2 K up to T_c in magnetic fields up to 15 T. Appl Supercond 1993;1:23 [DGM Informationsgesellschaft Verlag].
[59] Hampshire DP, Jones H, Mitchell EWJ. An in depth characterization of $(NbTa)_3Sn$ filamentary superconductor. IEEE Trans Magn 1985;21(2):289.
[60] Banno N, Takeuchi T, Tagawa K, Itoh K, Wada H, Nakagawa K. Field and temperature dependences of critical current density in rapid quenched and transformed Nb_3Al multifilamentary conductors. IEEE Trans Appl Supercond 2000;10(1):1026.
[61] Hampshire DP, Clark AF, Jones H. Flux pinning and scaling laws for superconducting V_3Ga. J Appl Phys 1989;66(7): 3160.
[62] Hampshire DP, Gray KE, Kampwirth RT. Scaling laws for the critical current density of NbN films in high magnetic fields. IEEE Trans Supercond 1993;3(1):1246.
[63] Zheng DN, Ramsbottom HD, Hampshire DP. Reversible and irreversible magnetization of the Chevrel-phase superconductor $PbMo_6S_8$. Phys Rev B 1995;52(17):12931.
[64] Cheggour N, Decroux M, Gupta A, Fischer Ø, Perenboom JAAJ, Bouquet V, et al. Enhancement of the critical current density in Chevrel phase superconducting wires. J Appl Phys 1997;81(9): 6277.
[65] Cheggour N, Decroux M, Fischer Ø, Hampshire DP. Irreversibility line and granularity in Chevrel phase superconducting wires. J Appl Phys 1998;84(4):2181.
[66] Ramsbottom HD, Hampshire DP. Flux penetration measurements and the harmonic magnetic response of hot isostatically pressed $(Pb,Gd)Mo_6S_8$. J Appl Phys 1999;85(7):3732.
[67] Kroeger DM, Easton DS, Koch CC, DasGupta A. In: Proceedings of the ICMC on Filamentary A15 Superconductors. New York: Plenum Press; 1980. p. 205.
[68] Ekin JW. Strain effects in superconducting compounds. Adv Cryog Eng 1984;30:823.
[69] Kramer EJ. Scaling laws for flux pinning in hard superconductors. J Appl Phys 1973;44(3):1360.

[70] Dew-Hughes D. Flux pinning mechanisms in type II superconductors. Philos Mag 1974;30:293.
[71] Kuroda T, Itoh K, Wada H, Togano K. A study on the relation between the strain scaling law and the temperature scaling law on flux pinning in Nb_3Sn superconducting wires. Cryogenics 2000; 40:287.
[72] Wördenweber R. A modified flux-line shear model: a possible mechanism of flux-line motion in high temperature superconductors. Cryogenics 1992;32(11):1099.
[73] Wördenweber R. Mechanism of vortex motion in high-temperature superconductors. Rep Prog Phys 1999;62:187.
[74] Ekin JW. Effect of transverse compressive stress on the critical current and upper critical field of Nb_3Sn. J Appl Phys 1987; 62(12):4829.
[75] Jakob B, Pasztor G, Bona M, Asner A. Reduced sensitivity of Nb_3Sn epoxy-impregnated cable to transverse stress. Cryogenics 1991;31:390.
[76] ten Haken B, Godeke A, ten Kate HHJ. A reversible rise in the critical current of a Nb_3Sn-bronze tape due to a transverse pressure. Inst Phys Conf Ser 1995;148:85.
[77] Kasaba K, Katagiri K, Shoji Y, Takahashi T, Watanabe K, Noto K, et al. Stress/strain dependence of critical current in Nb_3Sn superconducting wires stabilized with Cu–Nb microcomposites—effect of Nb content. Cryogenics 2001;41:9.
[78] ten Haken B, Godeke A, ten Kate HHJ. The strain dependence of the critical properties of Nb_3Sn conductors. J Appl Phys 1999; 85(6):3247.